Clay Minerals, (2018) **53**, 271–287

Direct Orange 34 dye fixation by modified kaolin

H. CHARGUI[1], W. HAJJAJI[2,*], J. WOUTERS[3], J. YANS[4] AND F. JAMOUSSI[1]

[1] *Laboratory Georessources, CERTE, BP 273, 8020 Soliman, Tunisia*
[2] *LabTEN Natural Water Treatment Laboratory, CERTE, BP 273, 8020 Soliman, Tunisia*
[3] *Department of Chemistry, University of Namur, 61 rue de Bruxelles, 5000 Namur, Belgium*
[4] *Department of Geology, ILEE, Institute of Life, Earth and Environment, University of Namur, 61 rue de Bruxelles, 5000 Namur, Belgium*

(*Received 7 June 2017; revised 5 April 2018; Associate Editor: Miroslav Pospíšil*)

ABSTRACT: The present study investigated the adsorption behaviour of Direct Orange 34, a highly toxic dye used in textile industries in Tunisia, on modified kaolinite-rich clays. A kaolin from the Sidi Bader (SDB) area was activated with hydrochloric acid to create the activated clay referred to hearafter as SDBa, or treated with $FeSO_4 \cdot 7H_2O$ to obtain its Fe-saturated form, Fe-SDB. The adsorbents were characterized by X-ray diffraction, X-ray fluorescence, transmission electron microscopy, BET surface area and zeta-potential measurements. The equilibrium adsorption data were analysed using the Langmuir and Freundlich isotherms. The estimated adsorption capacities (q_m) for the dye were improved in the Fe-loaded samples. The good fit ($R^2 = 0.99$) with a pseudo-second order expression suggests that the adsorption process could be effective following a chemisorption mechanism. At acidic pH, the optimum dye-retention rate was achieved for SDB (83%) after 60 min. The uptake decreased at neutral pH and increased again in alkaline media. This behaviour might be explained by the formation of covalent bonds between the OH radicals on the external surface and the negatively charged dye molecules. On the other hand, Fe impregnation increased the zeta potential of kaolinite, leading to a greater adsorption capacity compared to its natural and acid-activated counterparts. In addition, the adsorption rate increased when increasing the suspension temperature from 283 to 313 K. The modified kaolinite-rich materials showed satisfactory affinity for adsorbing this reactive dye.

KEYWORDS: kaolinite, Direct Orange 34, adsorption, modified clays, Tunisia.

Dyes are one of the world's most widespread pollutants; they react strongly with a large number of synthetic and natural surfaces in the textile, printing, dyeing, paper and plastics industries (Han *et al*., 2008; Shahid *et al.*, 2013). It is estimated that >100,000 types of synthetic dyes exist and >700,000 tons of dyestuff are produced annually worldwide (Robinson *et al*., 2001; Sun *et al*. 2009). In the textiles industry, up to 200,000 tons of dyes are lost in effluents every year during dyeing and finishing operations, due to inefficiency in recovery from the dyeing process and treatment (Ogugbue & Sawidis, 2011). Unfortunately, most of these dyes persist in the environment as a result of their high stability and low biodegradability (Couto, 2009). In addition, anti-microbial agents resistant to biological degradation are frequently used in the manufacture of textiles, particularly for natural fibres such as cotton (O'Neill *et al*., 1999; Couto, 2009). The synthetic origin and complex aromatic structure of these agents make them more resistant to biodegradation (Forgacs *et al*., 2004; Przystaś *et al*., 2012). Environmental legislation applies strict controls to dye-containing effluents before disposal into water pools

*E-mail: w.hajjaji@ua.pt
https://doi.org/10.1180/clm.2018.18

Copyright © Mineralogical Society of Great Britain and Ireland 2018
https://doi.org/10.1180/clm.2018.18 Published online by Cambridge University Press

(O'Neill *et al*., 1999; Ogugbue & Sawidis, 2011). Since the 1960s, increasingly severe environmental regulations have driven research in wastewater treatment and neutralization of solutions of reactive dyes (20–30% of the total dye market) (Orfao *et al*., 2006). Hence, several physical (Das & Basu, 2014), chemical (Liang *et al*., 2014) and biological (Pandey *et al*., 2007) methods have been developed to remove dyes and other coloured contaminants from wastewaters. Despite the effectiveness of the majority of these tests, the cost of the adsorbent and/or regeneration rate remain an important issue. In this context, the dye Direct Orange 34, commonly used in the Tunisian textiles industry, remains largely unstudied, and research focused on the treatment of wastewater derived is rare. Their high solubility, toxicity and carcinogenic effects make such reactive dyes difficult to remove; adsorption might be an attractive and efficient solution (Gurses *et al*., 2006; Chaari *et al*., 2015). This method involves a wide variety of materials including clays (Bhattacharyya *et al*., 2014), calcium carbonate and hydroxides (Vimonses *et al*., 2009), fly ash (Kumar *et al*., 2005), and Fe composites (Khosravi & Azizian, 2013). With the abundance of clay materials in Tunisia and the need for low-cost sorbents, recent work has reported the effective removal of organic pollutants by natural kaolinite, due to its layer structure and suitable mechanical and chemical stability (Errais *et al*., 2011; Hamdi & Srasra 2009).

Interest in using materials such as natural and modified kaolin as sorbents (Doğan *et al.,* 2009; Karaoğlu *et al*., 2010), catalysts (Khanikar & Bhattacharyya, 2013), membranes (Tahri *et al*., 2012) and fillers in the synthesis of polymer nanocomposites is growing, as is a new trend in wastewater treatment (Faria *et al*., 2012; Adebowale *et al*., 2008). Moreover, kaolins may be modified to improve their removal efficiency (Hajjaji *et al*., 2013; Akgül, 2014; Ugochukwu *et al*., 2014). In the present study, acid activation and Fe impregnation of the clay were applied to improve the dye-removal capacity. Furthermore, Fe-SDB is relatively stable and may be recycled because it can be recovered easily due to its magnetic properties.

MATERIALS AND METHODS

Materials and reagents

The clay (SDB) used in the present study was collected from the Sidi Bader quarry in Tabarka (NW Tunisia) (Fig. 1). The clay belongs to the Numidian Flysch located within the Kroumiries mountain chain (Moussi *et al*., 2011).

The chemical formula and UV-vis absorption spectrum of Direct Orange 34 are shown in Fig. 2. The maximum adsorption intensity was observed at $\lambda = 419$ nm. The stability of the dye and the colour intensity depend on the pH. The acid pH (3), and also the basic pH (10) influence the absorption spectrum of the dye as a new ultraviolet absorption band appeared at $\lambda = 227$ nm under these conditions. This phenomenon was also observed by Chaari *et al.* (2015). Stock dye solution (1 g L^{-1}) was prepared by dissolving 1 g of Direct Orange 34 in 1 L of deionized water and subsequently diluted to the required concentrations.

Mineralogical analysis of the SDB samples was carried out by X-ray diffraction (XRD, PANalytical X'PERT Pro diffractometer; Table 1). Oriented aggregates were treated with ethylene glycol and dried at 500°C for 2 h. The quantification of clay and associated minerals was evaluated from peak areas in the diffraction patterns (Zevin & Kimmel, 1995), and corrected by chemical data (López-Galindo *et al*., 1996). The experimental error was ± 5%. The chemical composition was determined by X-ray fluorescence (XRF) using an Axios Wavelength spectrometer. Loss on ignition was estimated by measuring the difference in weight in a 10 g sample after drying and after calcination at 1000°C. The microstructural characterization was performed by transmision electron microscopy (TEM, Phillips FEI-Tecnai 10 electron microscopy) with an accelerating voltage of 80 kV. The specific surface area and nitrogen adsorption/desorption isotherms were measured by the Brunauer Emmet Teller (BET) (1938) method using a MicromeriticsTristar 3000 instrument. Fourier-transform infrared (FTIR) spectra were collected using a Perkin Elmer Paragon 1000 Spectrometer. Peak assignments were made visually and with the Perkin Elmer *Spectrum*™ 10 spectroscopy software.

The surface zeta potential was evaluated using a Beckman Coulter, Delsa™ Nano C, particle analyser. The pH of dilute dispersions was adjusted to between 1 and 10 by adding either HCl or NaOH solutions, and measured directly before introducing the sample into the capillary cell. The cation exchange capacity (CEC) was estimated using the copper ethylenediamine complex method (Bergaya & Vayer, 1997).

To determine the particle-size distribution and the percentage of the <2 μm fine clay fraction, a Malvern Mastersizer 2000 laser particle size analyser was used. The range of particle sizes measured was between 0.02 μm and 2000 μm.

https://doi.org/10.1180/clm.2018.18 Published online by Cambridge University Press

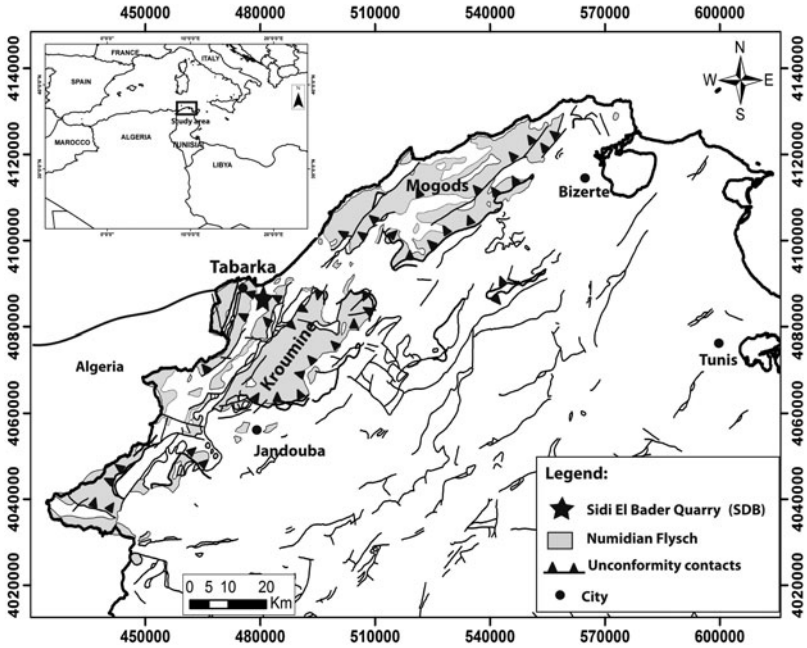


FIG. 1. Location of the clay deposit studied.

Acid-activated clay, referred to here as SDBa, was obtained by mixing, under vigorous stirring, 20 g of kaolin (SDB) with 100 mL of 2 M HCl solution for 1 h at 60°C, followed by aging at room temperature for 12 h. The precipitate was filtered and the treated material was washed several times with distilled water until pH 5. Finally, the product was dried in air at 60°C overnight.

For Fe loading, Fe-SDB was prepared by the impregnation method. 20 g of SDB powder was mixed with 100 mL of a 0.2 M iron sulfate ($FeSO_4.7H_2O$) solution for 3 h with a magnetic stirrer, and then aged for 12 h at room temperature (24 ± 2°C). A greater Fe concentration than this would lead to oversaturation and a decrease in the number of active adsorption sites. The cost of the reagent could be prohibitive when applied to wastewater treatment at an industrial scale. The suspension obtained was washed, centrifuged and dried overnight at 60°C and then calcined in a furnace at 400°C for 3 h.

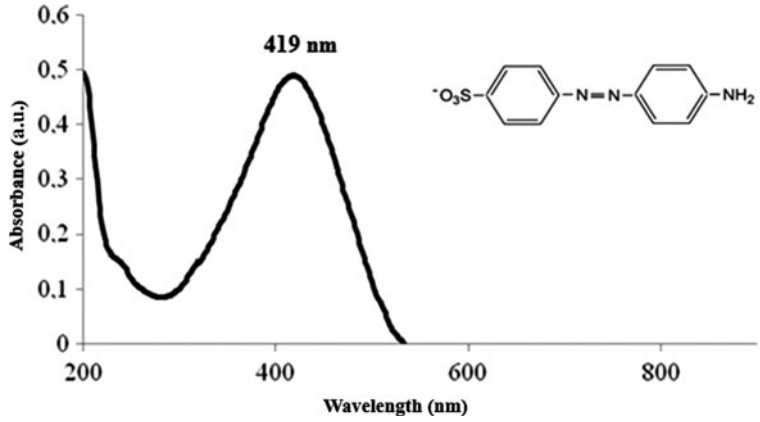


FIG. 2. Chemical structure of Direct Orange 34 with water solubility of 6 g/100 mL at 30°C; λ_{max} = 419 nm.

https://doi.org/10.1180/clm.2018.18 Published online by Cambridge University Press

Table 1. Composition, CEC and BET results of treated and untreated clays.

	Mineralogy (%)			Chemical composition (wt.%)	
	SDB	SDBa	Fe-SDB	SDB	
Kaolinite	57	+	+	SiO_2	56.5
Illite	8	+	+	Al_2O_3	28.0
Quartz	35	+	+	Fe_2O_3	1.42
Hematite	–	–	+		
	BET (m^2/g)	Pore volume (cm^3)	Pore size (Å)	CaO	0.19
SDB	23.4	0.0654	70.55	MgO	0.38
SDBa	33.85	0.0633	76.11	Cr_2O_3	0.03
Fe-SDB	31	0.055	84.34	ZrO_2	0.10
				P_2O_5	0.19
	CEC (meq/100 g)			LOI	9.75
SDB	3				

+: detected; –: not detected

Batch adsorption experiments were carried out by adding 0.5 g of clay to 50 mL of dye solution with an initial concentration of 200 ppm. The adsorption kinetics were studied by varying the contact time from 5 to 180 min. To study the effect of pH, the dye adsorption rate was measured while varying the pH from 3 to 10. The influence of temperature on dye adsorption was studied at 283, 298 and 313 K under optimum conditions for a 1 h contact time, *i.e.* 0.5 g of adsorbent and pH 3. The Direct Orange 34 adsorption isotherms were obtained by adding 1 g of clay to 100 mL of distilled water with various concentrations of dye (20, 30, 100, 150, 200 and 300 ppm) at acidic pH (3).

After adsorption, the suspension was centrifuged at 4000 rpm for 20 min and the supernatant was filtered under vacuum through 45 µm filters and was analysed using a SPECORD 205 spectrometer at a wavelength of 419 nm to determine the concentration of the residual dye. The amount of dye adsorbed by the SDB-based sorbent was determined by the following equation:

$$q_t = (C_0 - C_t)V/m \quad (1)$$

where C_0 and C_t are the initial and final (at time t) dye concentrations (mg L^{-1}), respsectively; q_t is the dye concentration on adsorbent at any time, t (mg g^{-1}), V is the volume of dye solution (L), and m is the mass of clay sample (g).

In this study, the Freundlich and Langmuir isotherm models (Freundlich, 1906; Langmuir, 1918) were applied. The linear form of Langmuir isotherm is given by the following equation:

$$C_e/q_e = 1/q_m b + C_e/q_m \quad (2)$$

where C_e is the equilibrium concentration (mg L^{-1}), q_e is the amount adsorbed at equilibrium (mg g^{-1}), q_m the maximum amount adsorbed (mg g^{-1}), and b is the energy of adsorption (Langmuir constant) (L mg^{-1}). The values of q_m and b were calculated from the slope and intercept of the linear plot C_e/q_e *vs.* C_e. The slope $1/q_m$ corresponds to the complete monolayer coverage (mg g^{-1}) and the intercept is $1/q_m b$ (plots not shown).

The Freundlich isotherm describes equilibrium on heterogeneous surfaces and, hence, does not assume monolayer capacity. The isotherm is described by the following equation:

$$q_e = k_F C^{1/n} \quad (3)$$

The logarithmic form of the equation becomes:

$$\log(q_e) = \log k_F + 1/n \log(C_e) \quad (4)$$

where k_F and n are Freundlich constants calculated from the slope and intercept of the Freundlich plot. An n value between 1 and 10 represents a good adsorption potential of the adsorbent (Freundlich, 1906).

The essential characteristics of the Langmuir equation can be expressed in terms of a dimensionless separation factor, R_L, which was defined by Hall *et al.* (1966) as:

$$R_L = 1/(1 + bC_0) \quad (5)$$

https://doi.org/10.1180/clm.2018.18 Published online by Cambridge University Press

where C_0 is the greatest initial dye concentration (mg L^{-1}) and R_L values indicate the shape of the isotherm.

The kinetic behaviour was studied using Lagergren pseudo-first order and pseudo-second order equations. The Lagergren pseudo-first order equation was used to fit the experimental results (Lagergren, 1898):

$$\mathrm{Ln}\,(q_e - q_t) = \mathrm{Ln}\,(q_e) - k_1 t/2.303 \quad (6)$$

where q_e and q_t are the amounts of Direct Orange 34 dye adsorbed per unit weight of adsorbent (mg g^{-1}) at equilibrium time and time t, respectively, and k_1 is the rate constant for the first-order kinetics. The adsorption rate constant was determined from the plot of $\ln(q_e - q_t)$ *vs*. *t*.

The pseudo-second order kinetics may be expressed as (Bhattacharyya & Sharma, 2004):

$$t/q_t = 1/k_2 q_e^2 + t/q_e \quad (7)$$

where k_2 is the rate constant of adsorption, q_e is the amount of dye adsorbed (mg g^{-1}) at equilibrium and q_t is the amount of dye adsorbed (mg g^{-1}) at time *t*.

The equilibrium adsorption capacity (q_e) and the second-order rate constant k_2 (mg g^{-1} min^{-1}) may be determined experimentally from the slope and intercept of plot of t/q_t *vs*. *t*, if the initial adsorption rate is (Gundogan *et al*., 2004):

$$h = k_2 q_e^2 \quad (8)$$

RESULTS AND DISCUSSION

Characterization of adsorbents

The natural SDB clay is composed mainly of kaolinite (57%) with minor amounts of illite (8%) (Table 1). Quartz is also abundant (35%), in good agreement with the large amount of SiO_2 reported by the chemical analysis (Table 1).

The XRD traces of the raw SDB clay, the acid-activated SDBa and impregnated Fe-SDB products are presented in Fig. 3. The basal reflections of kaolinite and illite appear at 7.23 Å (001) and 5.02 Å (002), respectively. The TEM images display the pseudo-hexagonal structure of kaolinite particles (Fig. 4a,b). After 1 h of acid activation, the position of the principal minerals' reflections remained unchanged. Nevertheless, a considerable decrease in peak intensities was observed, due to a decrease in the structural order of kaolinite under the effect of the acidic medium, also observed in TEM images (Fig. 4c,d). With acid activation, the clay minerals seem less crystalline and more agglomerated, in accordance with the increase in BET values (33.9 m^2/g) compared to the raw kaolin (23.4 m^2/g; Table 1). Acid activation opens the edges of the clay layers and increases the diameter of the pore (Ravichandran & Sivasankar, 1997; Chaari *et al*., 2009; Rezende & Pinto, 2016). During acid activation, exchangeable cations are initially replaced by protons, followed by partial dissolution of tetrahedral and octahedral sheets, creating new spaces. Acid sites formed at the layer edges contribute to the fixing of organic dye molecules (Komadel & Madejová, 2006).

The peak positions remained almost unchanged after Fe impregnation (sample Fe-SDB), although a slight decrease in peak intensities of kaolinite and illite was observed. This behaviour could be explained by the fixation of spherical Fe nanoparticles onto the clay minerals' surfaces (Fig. 4e,f). Fe treatment had the same effect on the specific surface area which was 31 m^2/g (Table 1).

The N_2 adsorption–desorption isotherms of SDB, SDBa and Fe-SDB are very similar to each other (Fig. 5). The treated and untreated clay are mesoporous materials characterized by type IV isotherms, typical of this type of clay (Michot *et al*., 1995). The physical properties derived from N_2 adsorption–desorption data are summarized in Table 1. The total N_2 adsorption uptake is slightly higher for SDBa and Fe-SDB than SDB. After the treatments, the BET surface area increased, probably due to the formation of surface cracks and defects as a result of the collapse of pore structure during Fe impregnation in Fe-SDB (Akgül, 2014), and acid activation (Rezende & Pinto, 2016) in SDBa. In SDBa, the specific surface area increased after acid activation due to the formation of mesopores; indeed, the total pore-volume values and mean pore diameters increased. Acid activation opens the edges of the clay layers and increases the diameter of the pores: consequently, specific surface area increases (Ravichandran & Sivasankar, 1997). The decreased pore volume and mean pore diameter of the Fe-SDB compared to the unmodified SDB suggest an increase in the microporosity, which might be ascribed to the opening of side pockets, or removal of some impurities included within the clay pores due to calcination (Gregg & Sing, 1982; Li, 2013).

The FTIR spectra were collected to obtain a better insight into the surface characteristics of the natural and modified clays (Fig. 6). All the kaolinite samples studied yielded FTIR spectra which correspond to those reported in the literature (Farmer *et al*.,

https://doi.org/10.1180/clm.2018.18 Published online by Cambridge University Press

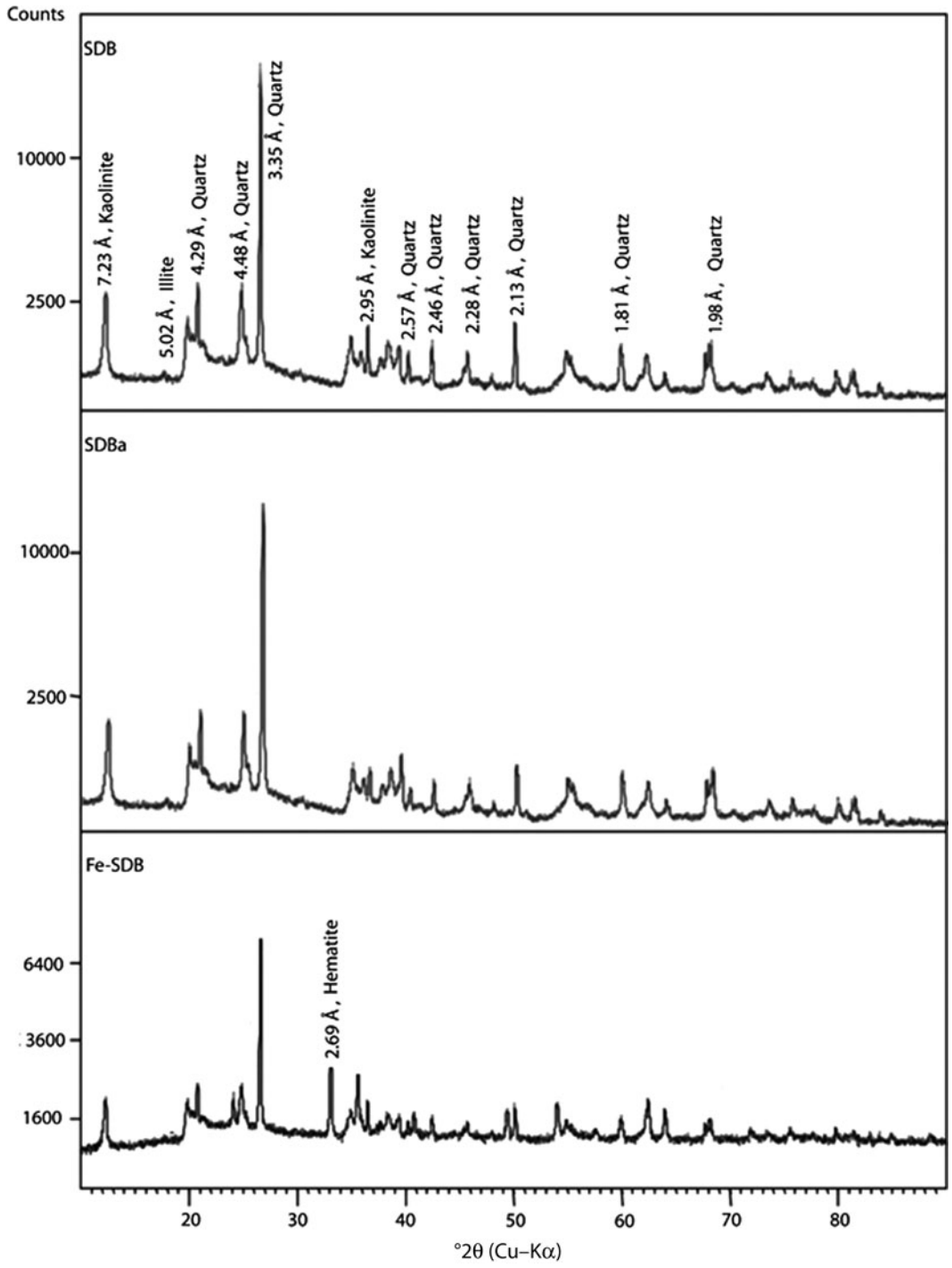


FIG. 3. XRD patterns of raw (SDB) clay, its acid-activated form (SDBa) and its Fe-impregnated form (Fe-SDB).

https://doi.org/10.1180/clm.2018.18 Published online by Cambridge University Press

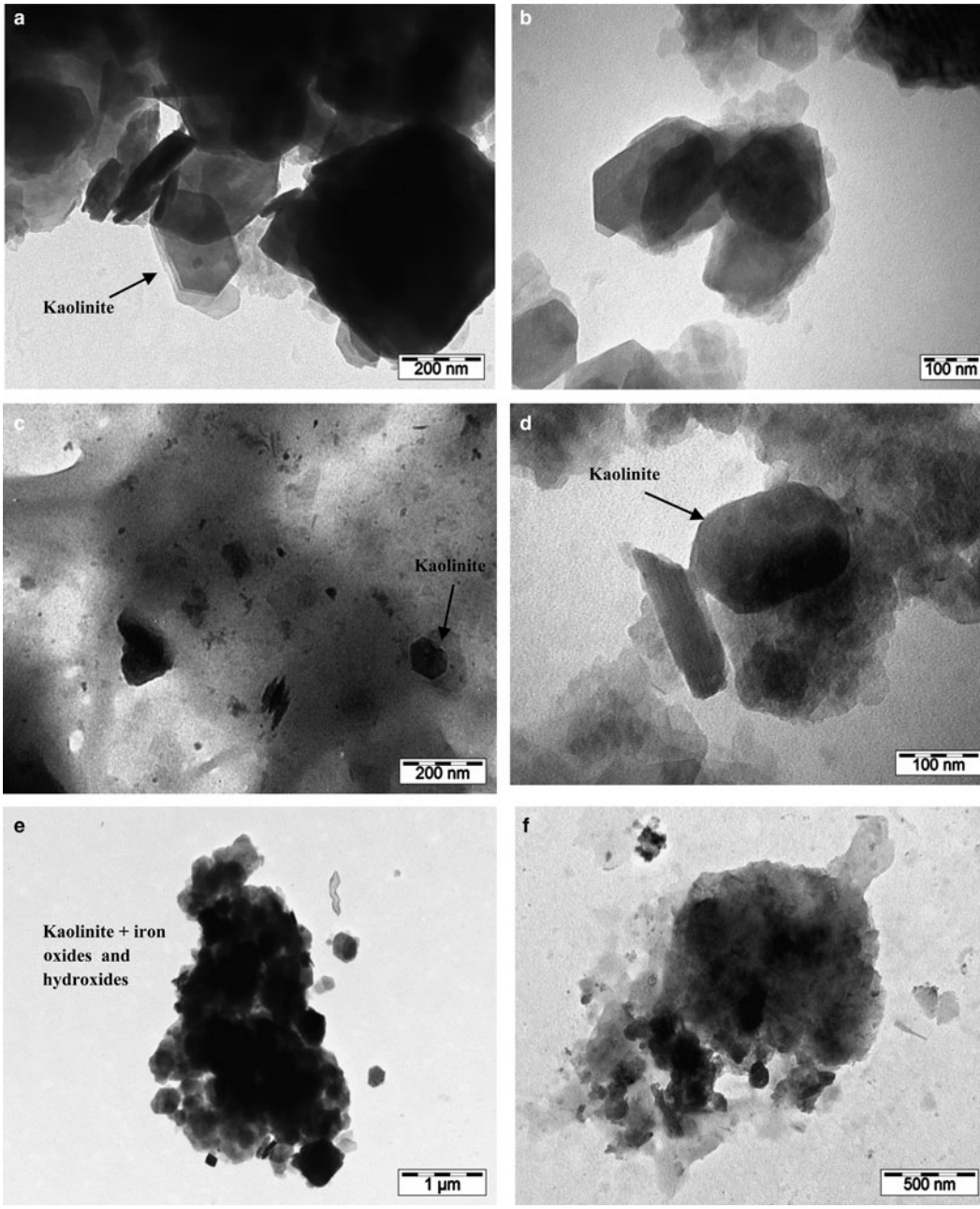


FIG. 4. TEM images of (a,b) SDB, (c,d) SDBa and (e,f) Fe-SDB clays.

1979; Madejová, 2003; Bhattacharyya *et al*., 2014). The following characteristic infrared bands were observed: O–Si–O stretching (1029, 1006 and 1114 cm^{-1}), Si–O bending (469 cm^{-1}), O–Si–O symmetric stretching (796 cm^{-1}), Al–OH bending (914 cm^{-1}), and vibrations of deformation of Al–O bonds and Si–O (689 cm^{-1}). Also, additional absorption bands appear in kaolinite in the OH-stretching region at 3618 cm^{-1}, due to inner OH groups lying between the tetrahedral and octahedral sheets, and at

https://doi.org/10.1180/clm.2018.18 Published online by Cambridge University Press

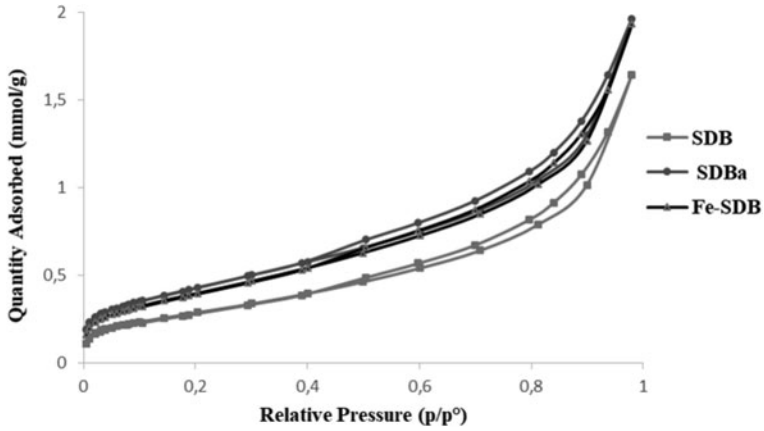


FIG. 5. Adsorption isotherms of the clays studied.

3695 cm^{-1}, assigned to in-phase symmetric OH stretching vibration (Madejová, 2003; Bhattacharyya *et al*., 2014). The bands at 524 and 734 cm^{-1}, corresponding to "pore opening" vibration and to symmetric stretching of free SiO_4, also appeared (Innocenzi *et al*., 2003; Akgül, 2014). In the Fe-SDB, the bands at 3618 and 1600 cm^{-1} were still present but exhibited increased intensity, suggesting the formation of additional Brønsted acid sites (new hydroxyl groups) by the incorporation of Fe^{3+} on the kaolinite (Li, 2013). Furthermore, bands corresponding to the typical frequencies for Fe-O (490, 599) were not observed, probably due to the overlap with the characteristic bands of kaolinite (Samanta *et al*., 2003; Guo *et al*., 2005).

The SDB and SDBa clays (Fig. 7) showed similar zeta potential profiles at acid and alkaline pH, which differ from the natural clay at medium pH (close to 20 mV at pH 7). At these levels, the modification in the clay surface charge due to acid activation (elimination of OH^- sites and fixation of H^+) was obvious.

In the case of Fe-SDB, there is a distinct behaviour of Fe species which leads to an increase in the zeta potential from –28.8 mV at pH = 10 to +40.3 mV at pH = 1, that may be explained on the basis of the charge neutralization *via* partial specific fixation of Fe^{3+} ions on the surface of the clay. The specific adsorption may be defined as the attraction of Fe^{3+} ions to the adsorbent surface by chemical forces in addition to electrostatic forces (Akgül, 2014). The formation of additional

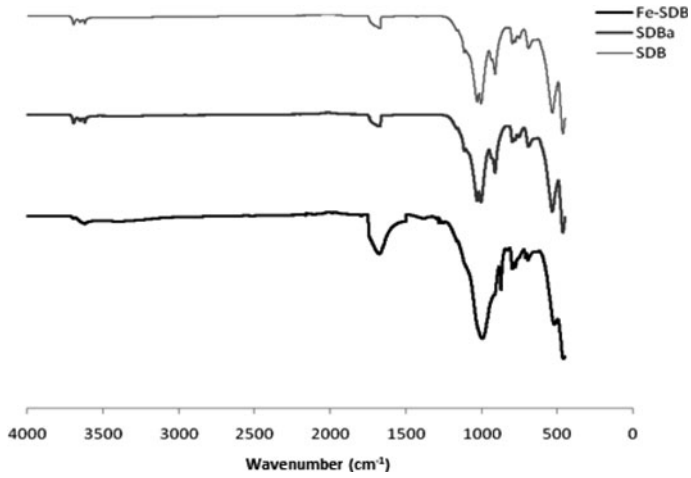


FIG. 6. FTIR spectra of the raw and modified clays.

https://doi.org/10.1180/clm.2018.18 Published online by Cambridge University Press

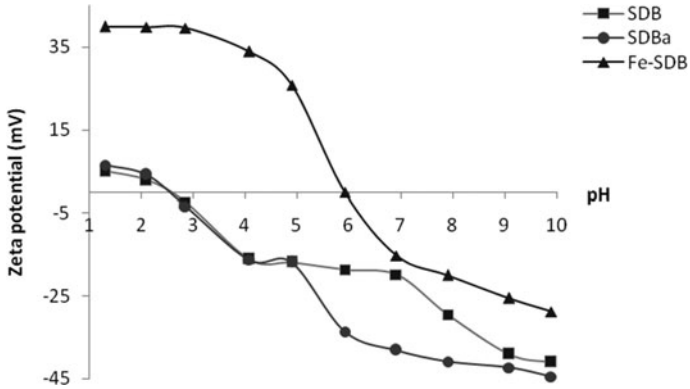


FIG. 7. Variation of zeta potential with pH.

hydroxyl groups (Fe-OH), which are protonated to form $Fe\text{-}OH_2^+$, may also increase zeta potential with decreasing pH (Gupta & Suhas, 2009).

Adsorption of ions and release of structural OH groups may modify the surface charge of clays (Akgül, 2014). The above reaction is forced by a charge-neutralization stable state that requires an equal number of equivalents of the adsorbed anion; the positive charge is neutralized, and as a result the hydroxyl group is released.

The proportion of the sample which was <2 μm was 57.5% for SDB, 41.5% for SDBa and 18.8% for Fe-SDB, according to the cumulative particle-size curve (Fig. 8). This reduction in the volume of the fine fraction (<2 μm) is explained by the agglomeration of the clay particles when treatment was applied.

Adsorption tests

The effects of parameters such as contact time, solution pH, initial dye concentration and solution temperature were studied to refine and optimize the removal process of Direct Orange 34 from laboratory-prepared aqueous solutions, using the previously prepared SDB, SDBa and Fe-SDB materials.

Contact time. The adsorption kinetics of Direct Orange 34 on the three clays (SDB, SDBa and Fe-SDB) were determined under the same operating conditions. The dye uptake for activated clay SDBa was relatively fast in the initial stage and equilibrium was reached after 15 min (Figs 9–11). Regarding SDB and Fe-SDB the maximum dye removal was obtained after 60 min of

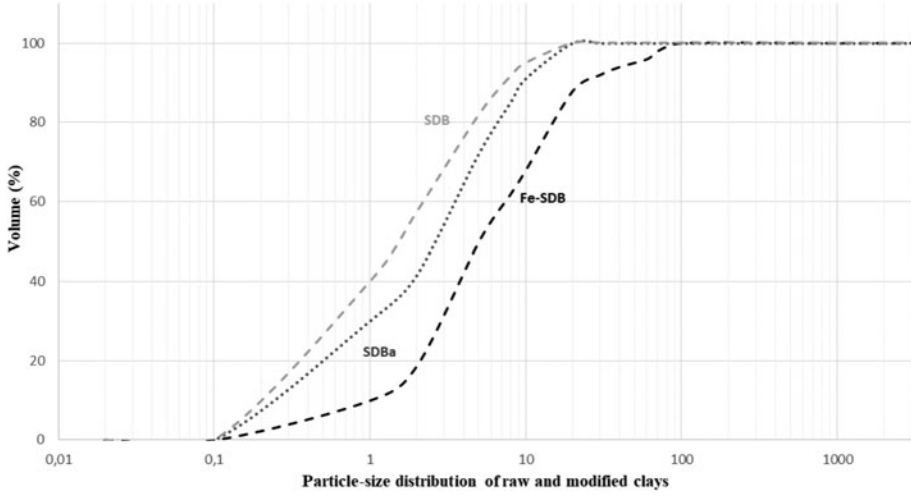


FIG. 8. Particle-size distribution of raw and modified clays.

https://doi.org/10.1180/clm.2018.18 Published online by Cambridge University Press

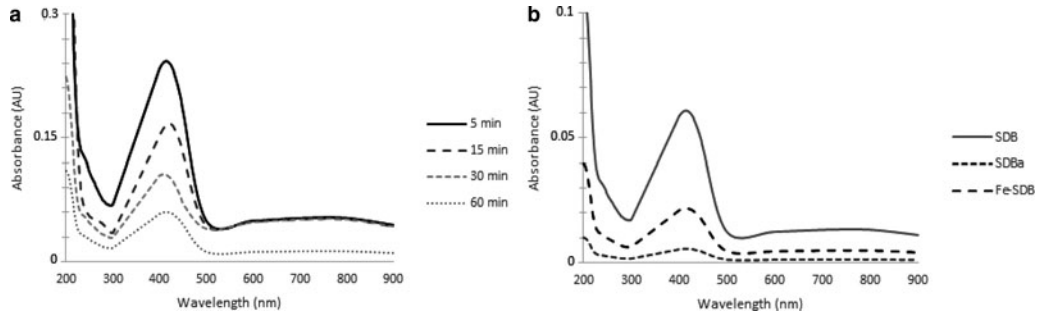


FIG. 9. (a) Evolution of the UV-vis absorption spectrum of Orange DO34 over time and after treatment with SDB clay; (b) absorption spectrum of Orange DO34 after treatment with SDB, SDBa and Fe-SDB.

contact time. The adsorption capacity of acid-activated kaolin (95% decolourization) was superior to the unmodified and Fe-impregnated kaolin (83% and 85%, respectively). This difference is mainly related to the greater availability of active sites on the SDBa clay surface.

At the chosen experimental conditions, unmodified SDB, with the lowest CEC value (Table 1), had a relatively high adsorption rate (83%). Therefore, cation exchange was probably not the main adsorption mechanism.

Variation in pH. The effect of pH on the adsorption of Direct Orange 34 is depicted in Fig. 12. The maximum adsorption capacity was observed over the pH range 3–5. The natural SDB clay displayed different adsorption behaviour; it decreased with increasing pH from 3 to 10, probably due to the protonation of the clay surface and electrostatic interaction between clay and dye molecules (Gurses *et al*., 2006; Errais *et al*., 2011). Similar behaviour was reported by Karaoğlu *et al.* (2010), who showed that the adsorption of reactive dyes on kaolinite is optimal at low pH (pH = 3), due to the potential of clay minerals to form bonds with H^+ and OH^- (Tahir & Rauf, 2006).

The substituents which render the Direct Orange 34 dye water soluble are sodium sulfonate groups (SO_3Na). In aqueous solutions, Direct Orange 34 ionizes into sodium cations and coloured sulfonate anions (Bulut *et al.,* 2008; Fungaro & Bruno, 2009; Chaari *et al*. 2015). The molcule of Direct Orange 34 also has an amine group (NH_2) at the end of the molecule, which may be protonated (NH_3^+) at low pH (Fu & Viraraghavan, 2001; Chaari *et al*. 2015), and might achieve greater basicity, which might result in an attraction between the protonated amine (NH_3^+) and the negatively charged functional groups of the adsorbent according to the following schematic raction:

$$R\text{-}SO_3Na + H_2O \rightarrow R\text{-}SO_3^- + Na^+$$

where *R* denotes the adsorbent surface. Moreover, zeta-potential measurements have shown that the isoelectric point, pH_{iep}, of kaolinite is at 2.35 (Alkan *et al*., 2005). The broken bonds along the surface of the clay crystals result in hydrolysis. In the acid medium, positive charges develop on the surface of the adsorbent, as shown in equation 9 (Dogan & Alkan, 2003; Dogan *et al*., 2004):

$$\equiv SO\text{-}OH + H^+ \leftrightarrows SO\text{-}OH_2^+ \quad (9)$$

The association of the dye anions with the positively charged kaolinite surface, resulting from the $SO\text{-}OH_2^+$ groups, might easily take place following equation 10:

$$\equiv SO\text{-}OH_2^+ + Dye^- \leftrightarrows SO\text{-}OH_2^+Dye^- \quad (10)$$

The adsorption capacity of SDB remained nearly constant in the pH range 3–7, decreasing at higher pH (Fig. 12). Although the negatively charged surface sites do not stimulate the adsorption of anionic dye (electrostatic repulsion), a significant amount of dye is removed (70% at pH 10). This suggests that a mechanism other than chemisorption may occur simultaneously. On the other hand, the adsorption capacity of the SDBa and Fe-SDB clays decreased remarkably beyond pH 5, reaching ~68% and 43%, respectively, at pH 7. At this stage, fewer available positively charged sites are present on the clay surface.

In alkaline media (pH > 8), the removal rate of the SDBa and Fe-SDB clays increased again. Normally, at high pH, competition between OH^- ions and dye anions is expected (Baskaralingam *et al*., 2006). However, in this case, a high decolourization of the solution was observed, proving that a more

https://doi.org/10.1180/clm.2018.18 Published online by Cambridge University Press

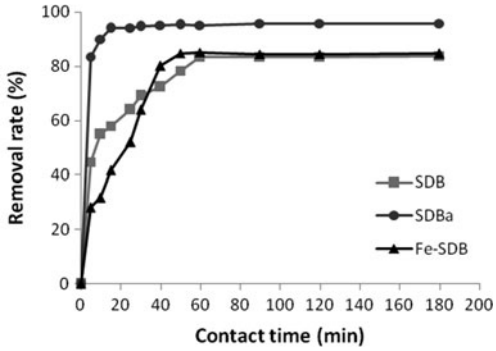


FIG. 10. Effect of contact time on the adsorption rate of dye on clay.

complex mechanism is in operation. At higher pH values, the formation of covalent bonds between the external surface –OH groups of Si and Al atoms of the adsorbent, and negatively charged dye molecules, might explain our observations. This behaviour has already been reported with some modified clays (Baskaralingam *et al*., 2006).

Temperature. The effect of temperature on adsorption capacity was investigated by assessing adsorption isotherms at various temperatures (283, 298, 313 K) at pH 3, using an initial dye concentration of 200 ppm (Fig. 13). From 283 to 313 K, the adsorption capacity for Direct Orange 34 increased, especially of the modified sorbents (from 46.6 to 50.8% for SDB, from 73.8 to 89.7% for Fe-SDB and from 84.3 to 93.6% for SDBa). This improvement in the dye-retention rate by SDBa might be due to the partial destruction of the kaolinite structure (Gonzalez-Pradas *et al.* 1998), and the specific adsorption of H^+ ions on the surface of kaolinite. As for Fe-SDB, the high retention rate might be attributed to the marked change in the surface charge caused by Fe impregnation (Fig. 7). With the modification of the clay-surface charge, the zeta potential increased from –2.4 mV to +39.6 mV at pH ≈ 3. Therefore, attractive forces between the adsorbent (Fe-SDB) and the dye molecules, and the number of available active sites, are expected to increase after impregnation of the Fe (Katranas *et al*., 2003).

The fact that the adsorption rate for Direct Orange 34 on unmodified and treated kaolinite increased with temperature should be due to an increase in the mobility of the dye with the increase in temperature (Singh, 1998; Tsai *et al*., 2004). An increasing number of molecules may also acquire sufficient energy to interact with active sites at the surface of the sorbent. This dependence on temperature of the amount of dye adsorbed may increase the ability of dye molecules (because of their larger diffusion coefficient) to approach the kaolinite surface. Therefore, it is suggested that the adsorption is an endothermic process (Dogan *et al*., 2006; Hu *et al*., 2006). Similar behaviour was observed by Akgül (2014) for the adsorption of the anionic dye, Congo Red, on clinoptilolite, and by Karaoğlu *et al.* (2010) for the adsorption of Reactive Blue 221 on kaolinite. However, these data contradict other studies (Chaari *et al*., 2015).

Initial dye concentration The removal efficiency of the materials decreased with decreasing dye concentration, close to the saturation equilibrium, to 14, 17.4 and 17.8 mg/g for SDB, SDBa and Fe-SDB, respectively (Fig. 14). At this level, greater competition between dye molecules at the active surface sites was reported at concentrations >200 ppm. Furthermore, in comparison to SDB, the acid-activated and Fe-impregnated sorbents exhibited more decolourization of the solution. With modification, the surface charge of the natural clay (SDB) became positive, as confirmed by the zeta potential (from –28 mV to + 39.6 mV at pH ≈ 3 for Fe-SDB). Therefore, the attractive forces between the adsorbent surface and the azo dye are expected to increase after incorporation of Fe (Katranas *et al*., 2003).

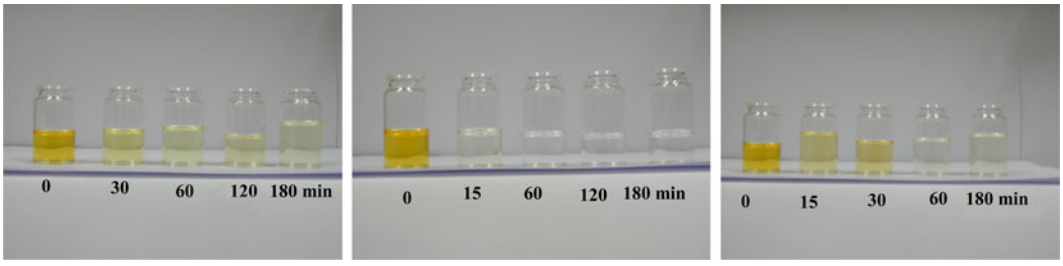


FIG. 11. Effect of contact time on the adsorption rate of dye on clay.

https://doi.org/10.1180/clm.2018.18 Published online by Cambridge University Press

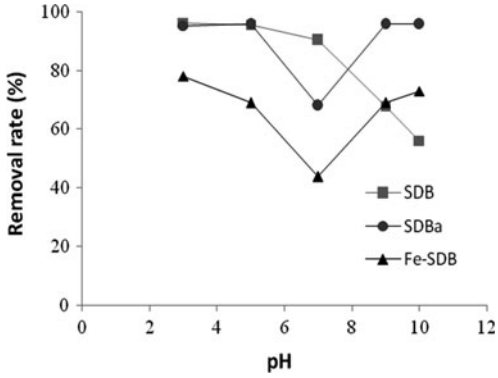


FIG. 12. The effect of pH on the adsorption rate of dye on clays.

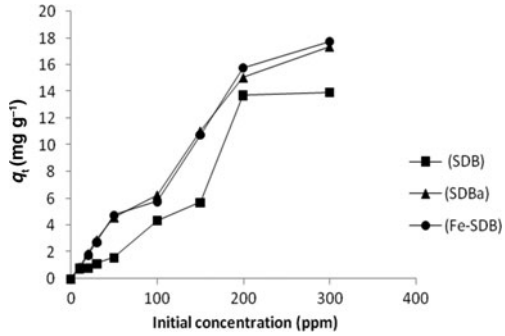


FIG. 14. Variation of the amount of dye adsorbed as a function of initial dye concentration.

Adsorption isotherms

The calculated Langmuir and Freundlich parameters are reported in Table 3. The experimental data fit better with the Langmuir adsorption isotherm model, as the values of coefficients of determination (R^2) are closer to 1. The Langmuir adsorption isotherm assumes that intermolecular forces decrease rapidly with distance, and that adsorption takes place at specific sites within the adsorbent. It is suggested that once the adsorbate occupies a site, no further adsorption takes place at that site (Bulut & Aydın 2006). Moreover, the adsorbent surface is structurally homogeneous, with identical adsorption sites, and energetically equivalent (monolayer sorption onto a surface). The value of the coefficient, R_L, indicates whether the isotherm is unfavourable ($1 < R_L$), linear ($R_L = 1$), favourable ($0 < R_L < 1$) or irreversible ($R_L = 0$). In the present study, the R_L values of 0.035 for SDB and 0.03 for SDBa indicated the applicability of the Langmuir isotherm, and confirmed a monolayer coverage of the Direct Orange 34 dye on the surface of natural and acid-activated SDB clays.

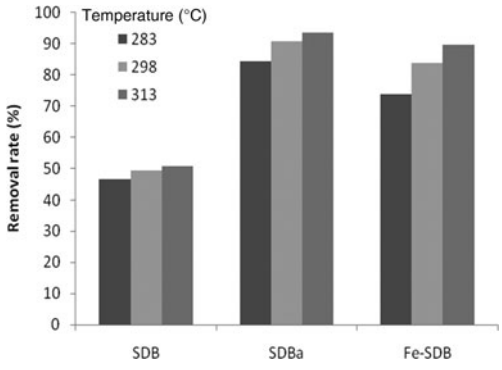


FIG. 13. Effect of the temperature on the adsorption rate of dye on clays.

Adsorption kinetics

The parameters calculated for the various kinetic models are given in Table 4. A very good fit ($R^2 = 0.99$) was obtained with the pseudo-second order model in relation to the linear variation of t/q_t as a function of time t. The calculated amount of dye adsorbed at equilibrium (q_e) is very close to the value obtained experimentally (Table 4). Thus, the adsorption of Direct Orange 34 on SDB, SDBa and Fe-SDB clays might be explained by the pseudo-second order kinetic model.

The q_m values of the adsorbents studied are also similar to, or greater than, those of the different dye-adsorbent systems listed in Table 2. However, the values are significantly smaller than the adsorption capacities achieved for commercial, coal-based mesoporous activated carbons (Nagarethinam & Mariappan, 2002; Gupta *et al*., 2004).

The best fit to the pseudo-second order kinetics indicates that the adsorption mechanism depends on the adsorbate and adsorbent (Vimonses *et al*., 2009), and the rate-limiting step may be chemisorption, involving valence forces through sharing or exchange of electrons (Errais *et al*., 2012; Natarajan *et al*., 2018). These results corroborate previous studies suggesting that kinetic adsorption of azo dyes on clay matches the pseudo-second order isotherm (Wang & Li, 2005; Li *et al*., 2009). As expected and reported in the N_2 adsorption-desorption isotherms study, the treated kaolins (SDBa and Fe-SDB) display greater uptake values resulting from the partial

https://doi.org/10.1180/clm.2018.18 Published online by Cambridge University Press

Table 2. Adsorption capacities of some dyes on various adsorbents.

Adsorbent	Adsorbate	q_e (mg g^{-1})	Reference
Commercial activated carbon	Congo Red	493.8	(Nagarethinam & Mariappan, 2002)
Fe-clinoptilolite	Congo Red	37	(Akgül, 2014)
Natural Tunisian clay	Reactive Red 120	9.3	(Errais *et al*., 2012)
Kaolin	Vert Nylomine	10.19	(Benguella & Yacouta-Nour, 2009)
Natural halloysite	Selophenyl TGL	9.60	(Chaari *et al*., 2015)
Natural kaolinite	Direct Orange 34	16.71	Present study
Acid-activated kaolin	Direct Orange 34	19.13	Present study
Fe-impregnated kaolin	Direct Orange 34	17.77	Present study

Table 3. Langmuir and Freundlich isotherms.

	Langmuir isotherms				Freundlich isotherms		
	Q_m	b	R_L	R^2	K_F	n	R^2
SDB	11.11	0.07	0.035	0.99	0.68	4.92	0.96
SDBa	17.88	0.11	0.030	0.97	1.69	1.952	0.92

destruction of kaolinite, and modification of the clay-surface charge due to acid activation (Gonzalez-Pradas *et al*., 1998) or Fe impregnation (Katranas *et al*., 2003).

SUMMARY AND CONCLUSIONS

The present study assessed the possible use of a Tunisian kaolin to remove Direct Orange 34, a common anionic dye, from aqueous solutions. The acid-activated kaolin (SDBa) and Fe-impregnated kaolin (Fe-SDB) are low-cost adsorbents for wastewater cleanup compared to other materials, such as activated carbon. Furthermore, Fe-SDB is relatively stable and can be reused as it can be recovered easily because of its magnetic properties. The untreated clay (SDB) retains slightly less dye than its modified counterparts. The removal of Direct Orange 34 by SDB and SDBa follows the Langmuir model. The greatest adsorption capacity achieved with modified SDB may be attributed to surface-protonation phenomena for SDBa, and to the charge reversal on the surface and the formation of new hydroxyl groups by the incorporation of Fe^{3+} for Fe-SDB. The adsorption kinetics of the reactive dye onto natural and modified SDB clay is quick, the equilibrium state being obtained

Table 4. Adsorption kinetic parameters for the Direct Orange 34 dye.

		Pseudo-first order			Pseudo-second order		
	Q_m (mg/g) (experimental)	k_1 (min^{-1})	Q_m (mg/g) (calculated)	R^2	k_2 (g/mg min)	Q_e (mg/g)	R^2
SDB	16.71	−0.06	12.20	0.87	0.01	17.30	0.99
SDBa	19.13	−0.07	3.27	0.74	0.13	19.19	0.99
Fe-SDB	17.77	−0.04	7.73	0.84	0.013	18.52	0.99

https://doi.org/10.1180/clm.2018.18 Published online by Cambridge University Press

after 15 min for SDBa and after 60 min for SDB and Fe-SDB. The adsorption profiles of all materials follow pseudo-second order models and may be described as chemisorption. The adsorption capacity increases with temperature suggesting endothermic binding phenomena between the adsorbate and adsorbents. The acidic pH enhances the dye removal due to electrostatic attraction, but >60% dye removal was still obtained at basic pH. This is indicative of the option to use the unmodified and modified SDB clays as alternative, low-cost adsorbents for the removal of Direct Orange 34 from industrial wastewaters (with pH 9–12). Thus, compared to the conventional adsorbents used, SDB clays are very promising from an industrial point of view due to their high capacity, local availability and low cost.

ACKNOWLEDGEMENTS

The authors are grateful to Wallonie-Bruxelles International, WBI, of Belgium for providing a grant as part of a cooperation project 'Valorisation des argiles naturelles' 2016–2018 (Axe 2 – projet 8). This work was co-financed by the MESRS (Tunisia) PJEC competetif Program - project 18PJEC02-03. B. Norberg, S. Davina Pierard, G. Rochez, B.-L. Su and V. Charles (University of Namur, Belgium), and S. Danthine and C. Bleeckers (University of Liège – AgroBioTech-Gembloux) are thanked for technical support. The authors also thank R.C. Pullar for improving the English in the manuscript.

REFERENCES

Adebowale K.O., Unuabonah E.I. & Olu-Owolabi B.I. (2008) Kinetic and thermodynamic aspects of the adsorption of Pb^{2+} and Cd^{2+} ions on tripolyphosphate-modified kaolinite clay. *Chemical Engineering Journal*, **136**, 99–107.

Akgül M. (2014) Enhancement of the anionic dye adsorption capacity of clinoptilolite by Fe^{3+} grafting. *Journal of Hazardous Materials*, **267**, 1–8.

Alkan M., Demirbas Ö. & Dogan M. (2005) Electrokinetic properties of kaolinite in mono and multivalent electrolyte solutions. *Microporous and Mesoporous Materials*, **83**, 51–59.

Baskaralingam P., Pulikesi M., Elango D., Ramamurthi V. & Sivanesan S. (2006) Adsorption of acid dye onto organobentonite. *Journal of Hazardous Materials*, **B128**, 138–144.

Benguella B. & Yacouta-Nour A. (2009) Elimination des colorants acides en solution aqueuse par la bentonite et le kaolin. *Science direct, C. R. Chimie*, **12**, 762–771.

Bergaya F. & Vayer M. (1997) CEC of clays: measurement by adsorption of a copper ethylenediamine complex. *Applied Clay Science*, **12**, 275–280.

Bhattacharyya K.G. & Sharma A. (2004) Azardirachta Indica leaf powder as an effective biosorbent for dyes: a case study with aqueous Congo red solution. *Environmental Management*, **71**, 217–229.

Bhattacharyya K.G., SenGupta S. & Kumar Sarma G. (2014) Interactions of the dye, Rhodamine B with kaolinite and montmorillonite in water. *Applied Clay Science*, **99**, 7–17.

Brunauer S., Emmett P.H. & Teller E. (1938) Adsorption of gases in multimolecular layers. *Journal of the American Chemical Society*, **60**, 309–319.

Bulut Y. & Aydın H. (2006) A Kinetics and thermodynamics study of Methylene Blue adsorption on wheat shells. *Desalination*, **194**, 259–267.

Bulut E., Ozacar M. & Ayhan Sengil I. (2008) Equilibrium and kinetic data and process design for adsorption of Congo Red onto bentonite. *Journal of Hazardous Materials*, **154**, 613–622.

Chaari I., Feki M., Medhioub M., Bouzid J., Fakhfakh E. & Jamoussi F. (2009) Adsorption of a textile dye "Indanthrene Blue RS (C.I. Vat Blue 4)" from aqueous solutions onto smectite-rich clayey rock. *Journal of Hazardous Materials*, **172**, 1623–1628.

Chaari I., Moussi B. & Jamoussi F. (2015) Interactions of the dye, C.I. direct orange 34 with natural clay. *Journal of Alloys and Compounds*, **647**, 720–727.

Couto S.R. (2009) Dye removal by immobilised fungi. *Biotechnology Advances*, **27**, 227–235.

Das L. & Basu J.K. (2014) Photocatalytic treatment of textile effluent using titania–zirconia nano composite catalyst. *Journal of Industrial and Engineering Chemistry*, **24**, 245–250.

Doğan M. & Alkan M. (2003) Adsorption kinetics of methyl violet onto perlite. *Chemosphere*, **50**, 517–528.

Doğan M., Alkan M., Türkyılmaz A. & Özdemir Y. (2004) Kinetics and mechanism of removal of methylene blue by adsorption onto perlite. *Journal of Hazardous Materials*, **109**, 141–148.

Doğan M., Alkan M., Demirbas O., Ozdemir Y. & Ozmetin C. (2006) Adsorption kinetics of maxilon blue GRL onto sepiolite from aqueous solutions. *Chemical Engineering Journal*, **124**, 89–101.

Doğan M., Karaoğlu M.H. & Alkana M. (2009) Adsorption kinetics of maxilon yellow 4GL and maxilon red GRL dyes on kaolinite. *Journal of Hazardous Materials*, **165**, 1142–1151.

Errais E., Duplay J., Darragi F., M'Rabet I., Aubert A., Huber F. & Morvan G. (2011) Efficient anionic dye adsorption on natural untreated clay: kinetic study and thermodynamic parameters. *Desalination*, **275**, 74–81.

Errais E., Duplaya J., Elhabiri M., Khodjac M., Ocampod R., Baltenweck-Guyote R. & Darragi F.

https://doi.org/10.1180/clm.2018.18 Published online by Cambridge University Press

(2012) Anionic RR120 dye adsorption onto raw clay: Surface properties and adsorption mechanism. *Colloids and Surfaces A: Physicochemical and Engineering Aspects*, **403**, 69–78.

Faria E.H., Ricci G.P., Marcal L., Nassar E.J., Vicente M. A., Trujillano R., Gil A., Korili S.A., Ciuffi K.J. & Calefi P.S. (2012) Green and selective oxidation reactions catalyzed by kaolinite covalently grafted with Fe(III) pyridine-carboxylate complexes. *Catalysis Today*, **187**, 135–149.

Farmer V.C., Fraser A.R. & Tait J.M. (1979) Characterization of the chemical structures of natural and synthetic aluminosilicate gels and sols by infrared spectroscopy. *Geochimica et Cosmochimica Acta*, **43**, 1417–1420.

Forgacs E., Cserháti T. & Oros G. (2004) Removal of synthetic dyes from wastewaters: a review. *Environment International*, **30**, 953–971.

Freundlich H.M.F. (1906) Over the adsorption in solution. *Journal of Physical Chemistry*, **57**, 385–471.

Fu Y. & Viraraghavan T. (2001) Fungal decolorization of dye wastewaters. *Bioresource Technology*, **79**, 251–262.

Fungaro D.A. & Bruno M. (2009) Removal of methylene blue from aqueous solution using zeolite synthesized from different coal fly ashes samples. *Química Nova*, **32**, 955–959.

Gonzalez-Pradas E., Villafranca-Sanchez M., Valverde-Garcia A. & Socias-Viciana M. (1998) Removal of tetramethyl thiuram disulphide from aqueous solution by chemically modified bentonite. *Journal of Chemical Technology and Biotechnology*, **42**, 105–112.

Gregg S.J. & Sing K.S.W. (1982) *Adsorption, Surface Area and Porosity, 2*. Academic Press, London.

Gundogan R., Acemioglu B. & Alma M.H. (2004) Copper (II) adsorption from aqueous solution by herbaceous peat. *Journal of Colloid and Interface Science*, **269**, 303–309.

Guo H., Zhang X., Cui M.H., Sharma R., Yang N.L. & Akins D.L. (2005) Magnetic ordering of ferric oxide within SiO_2-based mesoporous materials. *Materials Research Bulletin*, **40**, 1713–1725.

Gupta V.K. & Suhas (2009) Application of low-cost adsorbents for dye removal: A review. *Journal of Environmental Management*, **90**, 2313–2342.

Gupta V.K., Mittal A., Krishnan L. & Gajbe V. (2004) Adsorption kinetics and column operations for the removal and recovery of malachite green from wastewater using bottom ash. *Separation and Purification Technology*, **40**, 87–96.

Gurses A., Dogar C., Yalcin M., Akyildiz M., Bayrak R. & Karaca S. (2006) The adsorption kinetics of the cationic dye, methylene blue, onto clay. *Journal of Hazardous Materials*, **131**, 217–228.

Hajjaji W., Ganiyu S.O., Tobaldi D.M., Andrejkovičová S., Pullar R.C., Rocha F. & Labrincha J.A. (2013) Natural Portuguese clayey materials and derived TiO_2-containing composites used for decolouring methylene blue (MB) and orange II (OII) solutions. *Applied Clay Science*, **83–84**, 91–98.

Hall K.R., Eagleton L.C., Acrivos A. & Vermeulen T. (1966) Pore- and solid-diffusion kinetics in fixed-bed adsorption under constant-pattern. *Industrial Engineering Chemistry Fundamentals*, **5**, 212–223.

Hamdi N. & Srasra E. (2009) Retention of fluoride from industrial acidic wastewater and naf solution by three Tunisian clayey soils. *Research Report Fluoride*, **42**, 39–45.

Han R., Ding D., Xu Y., Zou W., Wang Y., Li Y. & Zou L. (2008) Use of rice husk for the adsorption of Congo red from aqueous solution in column mode. *Bioresource Technology*, **99**, 2938–2946.

Hu Q.H., Qiao S.Z., Haghseresht F., Wilson M.A. & Lu G.Q. (2006) Adsorption study for removal of basic red dye using bentonite. *Industrial and Engineering Chemistry Research*, **45**, 733–738.

Innocenzi P., Falcaro P., Grosso D. & Babonneau F. (2003) Order-disorder transitions and evolution of silica structure in self-assembled mesostructured silica films studied by FTIR spectroscopy. *Journal of Physical Chemistry B*, **107**, 4711–4717.

Karaoğlu H.M., Doğan M. & Alkan M. (2010) Kinetic analysis of reactive blue 221 adsorption on kaolinite. *Desalination*, **256**, 154–165.

Katranas T.K., Vlessidis A.G., Tsiatouras V.A., Triantafyllidis K.S. & Evmiridis N.P. (2003) Dehydrogenation of propane over natural clinoptilolite zeolites. *Microporous and Mesoporous Materials*, **61**, 189–198.

Khanikar N. & Bhattacharyya K. G. (2013) Cu(II)-kaolinite and Cu(II) montmorillonite as catalysts for wet oxidative degradation of 2 chlorophenol, 4-chlorophenol and 2,4-dichlorophenol. *Chemical Engineering Journal*, **233**, 88–97.

Khosravi M. & Azizian S., (2013) Adsorption of anionic dyes from aqueous solution by iron oxide nano-spheres. *Journal of Industrial and Engineering Chemistry*, **20**, 2561–2567.

Komadel P. & Madejová J. (2006) Acid activation of clay minerals. *Developments in Clay Science*, **1**, 263–287.

Kumar K.V., Ramamurthi V. & Sivanesan S. (2005) Modeling the mechanism involved during the sorption of methylene blue onto fly ash. *Journal of Colloid and Interface Science*, **284**, 14–21.

Lagergren S. (1898) About the theory of so-called adsorption of soluble substances. *Kungliga Svenska, Vetenskapsakad Handlingar*, **24**, 1–39.

Langmuir I. (1918) Adsorption of gases on plain surfaces of glass mica platinum. *Journal of American Chemical Society*, **40**, 1361–1403.

Li F. (2013) Layer-by-layer loading iron onto mesoporous silica surfaces: synthesis, characterization and

https://doi.org/10.1180/clm.2018.18 Published online by Cambridge University Press

application for As(V) removal. *Microporous and Mesoporous Materials*, **171**, 139–146.

Li Y., Gao B., Wu T., Wang B. & Li X. (2009) Adsorption properties of aluminum magnesium mixed hydroxide for the model anionic dye Reactive Brilliant Red K-2BP. *Journal of Hazardous Materials*, **164**, 1098–1104.

Li Y., Sun N., Li L., Zhao N., Xiao F., Wei W., Sun Y. & Huang W. (2013) Grafting of amines on ethanol-extracted SBA-15 for CO_2 adsorption. *Materials*, **6**, 981–999.

Liang C.Z., Sun S.P., Li F.Y., Ong Y.K. & Chung T.S. (2014) Treatment of highly concentrated wastewater containing multiple synthetic dyes by a combined process of coagulation/flocculation and nanofiltration. *Journal of Membrane Science*, **469**, 306–315.

López-Galindo A., Torres-Ruiz J. & Gonzalez López J.M. (1996) Mineral quantification in sepiolite-palygorskite deposits using X-ray diffraction and chemical data. *Clay Minerals*, **31**, 217–224.

Madejová J. (2003) FTIR techniques in clay mineral studies. *Vibrational Spectroscopy*, **31**, 1–10.

Michot C., Baril D. & Armand M. (1995) Polyimide-polyether mixed conductors as switchable materials for electrochromic devices. *Solar Energy Materials and Solar Cells*, **39**, 289–299.

Moussi B., Medhioub M., Hatira N., Yans J., Hajjaji W., Rocha F., Labrincha J.A. & Jamoussi F. (2011) Identification and use of white clayey deposits from the area of Tamra (northern Tunisia) as ceramic raw materials. *Clay Minerals*, **46**, 165–175.

Nagarethinam K. & Mariappan M. (2002) Adsorption of Congo red on various activated carbons. *Water, Air & Soil Pollution*, **138**, 289–305.

Natarajan S., Bajaj H.C. & Tayade R.J. (2018) Recent advances based on the synergetic effect of adsorption for removal of dyes from waste water using photocatalytic process. *Journal of Environmental Science*, **65**, 201–222.

O'Neill C., Hawkes F.R., Hawkes D.L., Lourenço N.D., Pinheiro H.M. & Delée W. (1999) Colour in textile effluents – sources, measurement, discharge consents and simulation: A review. *Journal of Chemical Technology and Biotechnology*, **74**, 1009–1018.

Ogugbue C.J. & Sawidis T. (2011) Bioremediation and detoxification of synthetic wastewater containing triarylmethane dyes by aeromonas hydrophila isolated from industrial effluent. *Biotechnology Research International*, doi: 10.4061/2011/967925.

Orfao J., Silva A., Pereira J., Barata S., Fonseca I. & Faria P. (2006) Adsorption of a reactive dye on chemically modified activated carbons – influence of pH. *Journal of Colloid and Interface Science*, **296**, 480–489.

Pandey A., Singh P. & Iyengar L. (2007) Bacterial decolorization and degradation of azo dyes. *International Biodeterioration & Biodegradation*, **59**, 73–84.

Przystaś W., Zabłocka-Godlewska E. & Grabińska-Sota E. (2012) Biological removal of azo and triphenylmethane dyes and toxicity of process by-products. *Water, Air & Soil Pollution*, **223**, 1581–1592.

Ravichandran J. & Sivasankar B. (1997) Properties and catalytic activity of acid modified montmorillonite and vermiculite clays. *Clay Minerals*, **45**, 854–858.

Rezende M.J.C. & Pinto A.C. (2016) Esterification of fatty acids using acid-activated Brazilian smectite natural clay as a catalyst. *Renewable Energy*, **92**, 171–177

Robinson T., McMullan G., Marchant R. & Nigam P. (2001) Remediation of dyes in textile effluent: a critical review on current treatment technologies with a proposed alternative. *Bioresource Technology*, **77**, 247–255.

Rouvier H. (1967) Sulfure et régime hydrodynamique du milieu de sédimentation. Exemple Tunisien: Le minerai de plomb du Koudiat Safra. *Mineralium Deposita*, **2**, 38–43.

Samanta S., Giri S., Sastry P.U., Mal N.K., Manna A. & Bhaumik A. (2003) Synthesis and characterization of iron-rich highly ordered mesoporous Fe-MCM-41. *Industrial & Engineering Chemistry Research*, **42**, 3012–3018.

Shahid M., Shahid-ul-Islam & Mohammad F. (2013) Recent advancements in natural dye applications: A review. *Journal of Cleaner Production*, **53**, 310–331.

Singh D. (1998) Effect of different factors on the adsorption of phosphamidon on two different types of Indian soil. *Adsorption Science and Technology*, **16**, 583–594.

Sun S.P., Li C.J., Sun J.H., Shi S.H., Fan M.H. & Zhou Q. (2009) Decolorization of an azo dye Orange G in aqueous solution by Fenton oxidation process: effect of system parameters and kinetic study. *Journal of Hazardous Materials*, **161**, 1052–1057.

Tahir S.S. & Rauf N. (2006) Removal of cationic dye from aqueous solutions by adsorption onto bentonite clay. *Chemosphere*, **63**, 1842–1842.

Tahri N., Masmoudi G., Ellouze E., Jrad A., Drogui P. & Amar R.B. (2012) Coupling microfiltration and nanofiltration processes for the treatment at source of dyeing-containing effluent. *Journal of Cleaner Production*, **33**, 226–235.

Tsai W.T., Lai C.W. & Hsien K.J. (2004) Adsorption kinetics of herbicide paraquat from aqueous solution onto activated bleaching earth. *Chemosphere*, **55**, 829–837.

Ugochukwu U.C., Jones M.D., Head I.M., Manning D.A. C. & Fialips C.I (2014) Effect of acid activated clay minerals on biodegradation of crude oil hydrocarbons. *International Biodeterioration & Biodegradation*, **88**, 185–191.

https://doi.org/10.1180/clm.2018.18 Published online by Cambridge University Press

Vimonses V., Jina B., Chow C. & Saint C. (2009) Enhancing removal efficiency of anionic dye by combination and calcination of clay materials and calcium hydroxide. *Journal of Hazardous Materials*, **171**, 941–947.

Vimonses V., Lei S., Jin B., Chow C.W.K. & Saint C. (2009) Kinetic study and equilibrium isotherm analysis of Congo red adsorption by clay materials. *Chemical Engineering Journal*, **148**, 354–364.

Wang S. & Li H. (2005) Dye adsorption on unburned carbon: kinetics and equilibrium. *Journal of Hazardous Materials*, **126**, 71–77.

Zevin L.S. & Kimmel G. (1995) *Quantiative X-ray Diffractometry.* Springer, New York.

https://doi.org/10.1180/clm.2018.18 Published online by Cambridge University Press